On the Emulation of Stiff Walls and Static Friction with a Magnetically Levitated Input/Output Device

S.E. Salcudean and T.D. Vlaar

Department of Electrical Engineering

University of British Columbia

Vancouver, BC, V6T 1Z4, Canada

April 3, 1996

Abstract

This paper addresses issues of mechanical emulation of stiff walls and stick-slip friction with a 6-DOF magnetically levitated joystick. In the case of stiff wall emulation, it is shown that the PD control implementation commonly used severely limits achievable wall damping and stiffness. It is also shown that the perceived surface stiffness can be increased without loss of stability by applying a braking force pulse when crossing into the wall.

For stick-slip friction, Karnopp's model was implemented using a PD controller within the stick friction threshold. Even though the PD controller allows some motion during the stick phase, the haptic feedback provided is remarkably similar to stick-slip friction.

1 Introduction

Although the idea of providing kinesthetic and touch feedback to the computer user has been put forward quite a while ago (Batter and Brooks, 1972) compared to the plethora of devices available for user input, *e.g.*, mice, joysticks, trackballs, graphics tablets and light pens, there are only a handful of commercial devices designed to provide kinesthetic and tactile feedback to the user. There are several reasons for the lack of such "haptic interfaces".

First, the computational requirements for haptic interface control are substantial and could not be satisfied with inexpensive microcontrollers until quite recently.

Second, only recently has there been any work in the design of high-performance mechanical systems usable as haptic interfaces. Examples include the systems designed by Iwata (Iwata, 1990, 1993) the magnetically levitated (maglev) joysticks designed by Hollis and Salcudean (Hollis et al., 1991, Salcudean et al., 1992, Hollis and Salcudean, 1992, Oh et al., 1993), the hand system designed at Harvard (Howe, 1992), the 4-DOF manipulandum developed at Northwestern University (Millmann et al., 1992), the 2-DOF manipulandum reported in (Adelstein and Rosen, 1992), the 2-DOF direct-drive "MagicMouse" (Kelley and Salcudean, 1993), the Queens Haptic Interface (Ellis, 1993).

Finally, little work on "mechanism emulation" through software control has been reported. In (Gotow et al., 1989), an apparatus with knobs with programmable

impedance was presented and used to study the effect of delays on impedance perception and the ability of subjects to resolve complex mechanical stimuli into the three basic components used in the test: stiffness, damping and inertia. The use of "virtual rectangles" generated with a direct drive robot in order to study kinesthetic perception was presented in (Mussa-Ivaldi et al., 1989) and (Hogan and Fasse, 1993). A number of issues arising in computer-generated force-feedback are addressed in reports of "sand-paper" and "molecular docking" experiments (Minsky et al., 1990), (Ouh-Young et al., 1989). A fair amount of work remains to be done in the simulation of interacting bodies and the presentation of virtual object trajectories in a stable way.

In addition, psychophysical studies are needed to determine required mechanism performance (frequency responses, motion range, etc.) and non-linear feedback control is needed to simulate interactions with a virtual environment in the presence of varying hand impedances.

This paper addresses the emulation of stiff walls and stick-slip motion. Simulation and experimental results are presented. The haptic interface used for this purpose is the UBC magnetically levitated (maglev) joystick (Salcudean et al., 1992) - a high frequency response, frictionless, back-drivable device with limited 6-DOF range.

Stiff wall emulation is difficult to achieve because, due to trade-offs between control performance and stability robustness, very stiff back-drivable systems that have a

Dimensions	Cylinder with $r = 66$ mm $h = 110$ mm
Stator mass	2 kg
Flotor mass	0.65 kg
Payload (continuous)	2 kg (along the z-axis)
Translation Range	$\pm$ 4.5 mm from center
Rotation Range	$\pm$ 6° from center
Resolution	< 5 μm (trans.) < 10 μrad (rot.)
Force/Torque Freq. Resp.	>3 kHz
Closed-Loop Position Freq. Resp.	>30 Hz (trans.) >15 Hz (rot.)
Actuator force constant	2 N/A
Max. continuous current	3 A / coil
Peak current	10 A / coil

Table 1: Summary of the UBC maglev joystick characteristics.

sufficient margin of stability to allow interaction with an operator are difficult to design. In this paper, it is argued that, for light, direct-drive devices with collocated actuation and sensing, the major limitation in the implementation of stiff walls by a common digital PD controller is the delay caused by data acquisition and control signal computation. Similar limitations have been noted in (Minsky et al., 1990), based on a phase margin argument, and in (Colgate et al., 1993), using a passivity argument, but the results in (Minsky et al., 1990) are optimistic while the results in (Colgate et al., 1993) are conservative.

It is also shown, through simulations and experimental results, that a remarkably effective way of increasing the *perceived* stiffness of a virtual wall in a stable manner is to add a "braking pulse" to the control signal upon penetration into the virtual wall. The braking pulse modifies the trajectory of the hand controller to make it closer to the trajectory generated when a real wall is encountered.

Stick-slip friction is emulated using a modification of Karnopp's friction model (Karnopp, 1985). Simulations and experiments show that the implementation provides a realistic feel.

This paper is organized as follows: Section 2 describes the UBC maglev joystick; Section 3 presents emulation results for stiff walls, Section 4 presents the emulation of stick-slip friction, while Section 5 provides a brief conclusion.

2 Experimental Setup

The UBC maglev joystick, designed by Salcudean using principles described in (Hollis et al., 1991), is used as the haptic interface. Its assembly sketch is shown in Figure 1 and its characteristics are given in Table 1.

The device has six Lorentz actuators, arranged in a star configuration with 120° symmetry. Each actuator consists of a flat coil immersed in the magnetic field of four rectangular magnets attached to permeable plates that contain the flux, and produces a force proportional to the current passing through it. In keeping with the terminology of (Hollis et al., 1991), the actively levitated joystick handle is referred to as the "flotor". The location of the flotor with respect to the stator is detected by sensing the projections of three narrow beam LEDs on the surfaces of three two-dimensional Position Sensing Diodes, as described in (Hollis et al., 1991). The actuator coils are driven by current drivers each having a maximum continuous current of 10 A.

The maglev joystick flotor is kept in controlled "flight" by a VME-based SPARC^{TM} processor running the VxWorks^{TM} real-time operating system, and associated input-output cards. A Silicon Graphics workstation is used for graphical display and communicates with the haptic interface control processor via a serial link.

By comparison to the maglev wrists presented in (Hollis et al., 1991, Oh et al, 1993), that use coils arranged on the faces of a hexagonal cylindrical shell, the UBC wrist is substantially smaller, although it can produce the same forces and only slightly

reduced torques.

Since the Lorentz actuators are current controlled to about 2 kHz, while the first vibration modes in the flotor occur at about 1 kHz, for the experiments presented in this paper, the UBC maglev joystick flotor can be modelled as a single controlled rigid mass, of mass $m = 0.7$ kg. With the present current amplifiers, the maximum force along vertical axis is 60 N.

3 Stiff Wall Emulation

A model of a hand-held joystick flotor interacting with a stiff wall is given by

$$m\ddot{x} = f_h + f_{wall} = f_h - b_e\dot{x} - k_e x \qquad \text{if } x \leq 0 \tag{1}$$

$$= f_h \qquad \text{if } x > 0 \tag{2}$$

where x is the mass displacement, k_e is the wall stiffness and b_e is the wall damping. The hand force f_h can be thought of as having an exogenous "active" component that depends on the mass position and the force desired by the operator, and a "passive" component that depends on x and the hand impedance.

The experimental evidence of the authors suggests that the operator hand impedance has a stabilizing effect on the flotor, since the hand acts primarily as a damper for small motion of the hand controller. Since the human impedance interacts with the flotor in a manner that is difficult to quantify (it depends on the grip, arm extension,

etc.), it makes sense to consider first the emulation of a stiff wall when the flotor is pushed by a constant force, that, if it could be isolated, would correspond to the active component f_h of the hand force. This can be implemented in a controllable way by "dropping" the flotor, under gravitational forces, onto the emulated stiff surface. Clearly, a stable behaviour is required since it is a limiting case for a very light grip.

For a surface modelled by a spring-damper system as in (1), a rigid body dropped on it from a given height bounces only if the surface damping coefficient $\rho = \frac{b_e}{2\sqrt{k_e}} < 1$ (otherwise, a response without overshoot would result). If $\rho < 1$, it can be shown by integrating $\dot{x}^2$ between crossings into and out of the wall, that the coefficient of energy restitution to the rigid mass for every bounce against the stiff surface is given by $r = \exp(-\frac{2\pi\rho}{\sqrt{1-\rho^2}})$, which exhibits a sharp decrease from 1 even for very small ρ ($r < 0.2$ for $\rho > 0.1$). Since the energy of a dropped object decreases exponentially in r with the number of bounces, it is clear that a rigid object dropped on most surfaces should reach continuous contact in a very short time. This is obviously supported by experience with most real objects and surfaces. Since very little damping inside an ideal stiff wall makes the contact oscillations die out very quickly, it must be that the common implementations of stiff walls do not provide sufficient damping *inside* the wall. This indicates that the instability problem noted in haptic interfaces is not a "contact" instability, but, rather a question of instability within the stiff wall.

The stiff wall component of (1) is usually implemented by a digital PD controller,

using a first-order finite difference approximation of the velocity term

$$f_{wall\,k} \;\; = \;\; -k_p x_{k-1} - \frac{k_v}{T}(x_{k-1} - x_{k-2}) \;\; , \tag{3}$$

where $1/T$ is the sampling frequency and the notation $s_k = s(kT)$ is used for any signal s. In terms of z-transforms, the above equation becomes

$$F_{wall}(z) \;\; = \;\; -(k_p + \frac{k_v}{T})\frac{1}{z}X(z) + \frac{k_v}{T}\frac{1}{z^2}X(z) \;\; , \tag{4}$$

while the transfer function model of the mass is

$$X(z) = \frac{T^2}{2m}\frac{z+1}{(z-1)^2}[F_{wall}(z) + F_h(z)] \;\; . \tag{5}$$

Combining (5) with (4) leads to a closed-loop characteristic polynomial given by

$$\chi(z) = z^4 - 2z^3 + (1 + c_p + c_v)z^2 + c_p z - c_v \;\; , \tag{6}$$

where the non-dimensional "stiffness" and "damping" are given by

$$c_p = \frac{T^2}{2m}k_p \qquad\qquad c_v = \frac{T}{2m}k_v \;\; . \tag{7}$$

The level sets of the maximum absolute values of the roots of $\chi(z)$ can be plotted *vs* the non-dimensional coefficients c_p and c_v and are shown in Figure 2. They show fundamental limitations on the achievable "virtual" stiffness and damping with the controller (3). For example, with $m = 0.7$ kg and $1/T = 200$ Hz, the maximum k_p in (3) is approximately 3900 N/m, and is achieved with a value of k_v in (3) of approximately 60 N/(m/s). Furthermore, the interpretation of k_p and k_v as virtual

stiffness and damping is incorrect. An ideal analog controller implementing (1) with k_e=3900 N/m and b_e=60 N/m would produce an underdamped response that settles very fast after a reasonable overshoot, while the discrete implementation (3) would lead to a marginally stable system.

It is important to note that, unlike in previously reported work, the model (3) includes a one-sample delay between the position signal and the applied force. Such a delay often occurs in practice, as the control sampling rate is increased to the maximum that allows the control signal to be computed from measurements, and does not allow full placement of the closed-loop (discrete-time) system poles.

Instead of applying the control law (3), a better design approach would be to add a pole at the origin of the model (5) to include the computational delay, and then perform a robust, observer-based discrete-time controller design. This would allow arbitrary pole placement and a tradeoff of wall stiffness *vs* robustness to disturbances and model errors, *e.g.*, hand forces and impedances. This approach was pursued by the authors and presented in (Vlaar, 1994), but did not result in substantially higher wall stiffness.

In this paper, a different approach to increasing the perceived wall stiffness is presented and leads to excellent results. The approach is motivated by the fact that an object colliding with a very stiff surface would stop almost instantly upon impact. Accordingly, upon impact with the virtual wall, the mass should be brought to zero

velocity as fast as possible, *i.e.*, during one control period. Providing that the required force does not saturate the actuator, the "braking pulse" from velocity $v(kT)$ to zero velocity (again, assuming constant force between control samples) can be calculated as

$$f_{pulse} = m(v_k - v_{k-1})/T = -mv_{k-1}/T \ . \tag{8}$$

This corresponds to very high damping upon wall penetration, and, for $x_{k-1} < 0$, can be implemented as

$$\begin{aligned} f_{wall_k} &= -(k_{pulse} + k_v/T)(x_{k-1} - x_{k-2}) \qquad \text{if } x_{k-2} > 0 \text{ and } x_{k-1} \leq 0 \\ f_{wall_k} &= -k_p x_{k-1} - \frac{k_v}{T}(x_{k-1} - x_{k-2}) \qquad \text{otherwise,} \end{aligned} \tag{9}$$

where $k_{pulse} + k_v/T = m/T^2$. Because the additional high damping only occurs on the wall surface, it does not have a de-stabilizing effect, since it is impossible to hold the flotor exactly on the emulated wall edge. If, due to actuator saturation, the braking pulse is limited in magnitude, the additional braking control action can be applied over a number of control samples. The magnitude of the braking pulse can be computed in a similar manner.

The fall of the flotor onto a virtual stiff wall was simulated in Matlab^{TM} and Simulink^{TM}, using a hybrid continuous (flotor dynamics) - discrete (controller) system. The controller simulation used (9), running at $1/T = 200$ Hz, but was implemented with one less delay than shown in (9), (*i.e.*, with $k := k + 1$ on the right

hand side of (9)), a transport delay of $\Delta T = 0.0015$ s, and a reduced pulse width for the braking force (0.003 seconds instead of 0.005 seconds). This closely matches the A/D conversion - control computation - D/A conversion cycle, as the control processor performs other tasks (variable monitoring, I/O, etc.) after sending new current values to the D/A board, and allows for the slew-rate of the coil drivers. The results, with gains $k_p = 6000$ N/m, $k_v = 80$ N/(m/s) and $k_{pulse} = 220$ N/(m/s) are shown in Figure 3.

A phase-plane plot displaying simulated flotor trajectories is shown in Figure 4. For comparison, a simulation of a fully analog system implementing (1) with $k_e = k_p$, $b_e = k_v$, is also shown (a 10 kHz low-pass filter is applied to the control signal to make it realizable).

The experimental data with the same mass, control rate and gains is shown in Figure 5. Data collected while an operator manipulates the flotor against the virtual wall is shown in Figure 6.

The braking pulse applied to the flotor on surface crossing is perceived similarly to hitting a hard surface, and even generates an audible effect and vibration on the computer table on which the joystick rests. Although no careful psychophysical analysis was performed, many operators had difficulty differentiating between the virtual wall and the metal stator that mechanically limits the flotor range. No stability problems, nor chattering, were encountered.

4 Stick-Slip Friction

The emulation of stick-slip friction could be an extremely useful feature in a haptic interface. For example, an object could be positioned on the screen and frozen there without separate operator intervention such as key strokes, mouse-button clicks, etc.. In a joystick controlling a slave robot, stick-slip friction would allow switching to position from rate mode without the slave being returned to a null position when the operator releases the control.

The emulation presented in this paper uses a slightly modified version of Karnopp's model (Karnopp, 1985). According to Karnopp's model, a mass sliding on a surface with stick-slip friction could be in two states. If STUCK, any external force f_{ext} acting on the mass with $|f_{ext}| < f_{max}$ is balanced exactly and the mass remains in the STUCK state. If the external force magnitude exceeds f_{max}, the mass state changes to SLIDING. While in the SLIDING state, a damping force $-k_v\dot{x}$ is exerted. The condition for transition from the SLIDING to STUCK state is $|\dot{x}| < v_{min}$, where v_{min} is a small threshold velocity.

The equations of motion are:

$$
\begin{aligned}
m\ddot{x} &= f_{ext} - k_v\dot{x} + f_{stick} \qquad (10)\\
f_{stick} &= -f_{ext} \qquad \text{if STUCK}\\
f_{stick} &= 0 \qquad \text{if SLIDING}
\end{aligned}
$$

with the state change being governed by

$$\begin{array}{c} |f_{ext}| > f_{max} \\ \longrightarrow \\ \text{STUCK} \qquad\qquad\qquad \text{SLIDING} \\ \longleftarrow \\ |\dot{x}| < v_{min} \end{array} \tag{11}$$

Stiction forces cannot be emulated precisely with a frictionless mechanism, as the mechanism would have to have infinite gain position feedback or perfect force tracking. Instead, a PD controller can be used to emulate stick-slip friction as follows:

$$\begin{aligned} m\ddot{x} &= f_{ext} - k_v\dot{x} + f_{stick} \qquad (12) \\ f_{stick} &= k_p(x_{STUCK} - x) \qquad \text{if STUCK} \\ f_{stick} &= 0 \qquad\qquad\qquad\quad \text{if SLIDING} \end{aligned}$$

$$\begin{array}{c} |k_p(x_{STUCK} - x)| > f_{max} \\ \longrightarrow \\ \text{STUCK} \qquad\qquad\qquad \text{SLIDING} \\ \longleftarrow \\ |\dot{x}| < v_{min} \end{array} \tag{13}$$

(set $x_{STUCK} = x$ upon transition)

In one of the experiments used to evaluate stick-slip friction emulation, f_{ext} was implemented as a virtual spring force $f_{ext} = k_s(x_s - x)$ with stiffness $k_s = 1000$ N/m and center $x_s = 3$ mm. Karnopp's model for this experiment and its emulation are

shown in Figure 7. The spring was triggered at time $t = 0$ seconds against the resting (*i.e.*, flown in STUCK state) flotor mass. The position and velocity of the flotor mass are displayed against the Karnopp model simulation in Figure 8. The gains and thresholds used were $k_p = 6000$ N/m, $k_v = 80$ N/(m/s), $v_{min} = 5$ mm/s, and $f_{max}= 2$ N. The control rate was $1/T = 200$ Hz. It can be seen that the motion of the flotor closely approximates that simulated by Karnopp's model. The oscillations of the flotor in the STUCK position could be reduced substantially with a higher control rate. The initial velocity undershoot (time $t = 0.05$ seconds) is due to the increased restoring force $k_p(x_{STUCK} - x)$ as the flotor is pushed out of its STUCK state. As there will always be a finite slope force *vs* position curve holding the flotor in its STUCK case, it is unlikely that this overshoot can be eliminated with better control.

Figure 9 compares plots of the actual flotor position and x_{STUCK} as the joystick flotor is manipulated by an operator (all six axes are controlled in stick-slip mode for this experiment). Each change in value of x_{STUCK} represents a stick-sliding-stick transition. With the parameter values given above, the operator can control the flotor position with a resolution of about 0.33 mm. A higher position gain and smaller force threshold would allow much finer granularity.

5 Conclusions

This paper presented simulation and experimental results on the emulation of stiff walls and static friction for haptic interfaces. The UBC maglev joystick was used for this purpose.

The problem of dropping a rigid mass on a stiff virtual wall was considered as a way of obtaining controlled results, independent of hand impedance. Based on the coefficient of energy restitution, it was argued that the stability problem frequently encountered when dealing with stiff walls is not due to changes in dynamics on the wall border, but rather due to the high stiffness that has to be achieved within the wall. It was shown that the most common discrete PD control implementation does not allow full placement of the discrete system closed-loop poles and leads to counter-intuitive and oscillatory behaviour. It was also shown that the perceived stiffness of virtual walls can be increased in a stable fashion by adding a braking pulse to the control force when crossing into the wall.

The emulation of stick-slip friction was also considered. Karnopp's model was combined with a PD controller to hold the joystick in the stuck position. The approach was demonstrated to work by simulations and experiments. Stick-slip friction allows positioning of a joystick within its workspace in a stable manner and with a controllable resolution and could be extremely useful in position controlled teleoperation or manipulation of virtual objects.

Overall, the quality of mechanism emulation with the UBC maglev joystick is excellent (stiffness ranges of 6 N/m to 10,000 N/m have been obtained). The only drawback of the device is its small motion range. For larger motion range, a macro-micro approach is being presently pursued by the authors. The significant influence of sampling time on the performance of the UBC maglev joystick suggests that designers of haptic interfaces should look towards collocated sensing and high-speed actuation.

6 References

Adelstein, B.D. and Rosen, M.J., 1992. Design and Implementation of a Force Reflecting Manipulandum for Manual Control Research. In *Advances in Roboics*, volume ASME-DSC 42, pages 1–12.

Colgate, J.E., Grafing, P.E., Stanley, M.C., and Schenkel, G., 1993. Implementation of stiff virtual walls in force-reflecting interfaces. In *IEEE Virtual Reality annual international Symposium*, pages 202–208.

Ellis, R.E., Ismaeil, O.M., and Lipsett, M.G., 1993. Design and evaluation of a high-performance prototype force-feedback motion controller. In H. Kazerooni, J.E. Colgate, and B.D. Adelstein, editors, *Advances in Robotics, Mechatronics and Haptic Interfaces, 1993*, ASME, New York, pages 55–64.

Gotow, J.K., Friedman, M.B. and Nagurka, M.L. Controlled impedance test apparatus for studying human interpretation of kinesthetic feedback. In *Proceedings of*

the 1989 American Control Conference, pages 332–337, Pittsburgh, PA., June 21-23 1989.

Karnopp, D., 1985. Computer simulation of stick-slip friction in mechanical dynamic systems. *ASME Journal of Dynamic Systems, Measurement and Control*, Vol. 107, pp.100–103.

Kelley, A.J. and Salcudean, S.E., 1993. Magicmouse: tactile and kinesthetic feedback in the human-computer interface using an electromagnetically actuated input/output device. Submitted for publication in the *IEEE Trans. on Robotics and Automation*, Jan. 1993., conditionally accepted for publication.

Hogan, N. and Fasse, E.D.. Quantitative assessment of human perception of virtual objects. In *Proceedings of the 1993 ASME Winter Annual Meeting*, volume ASME-DSC 49, pages 89–97, New Orleans, LA, 1993.

Hollis, R.L., Salcudean, S.E., and Allan, P.A., 1991. A Six Degree-of-Freedom Magnetically Levitated Variable Compliance Fine Motion Wrist: Design, Modelling and Control. *IEEE Trans. Robotics Automat.*, Vol. 7, pp.320–332.

Hollis, R.L. and Salcudean, S.E., 1992. Input/output system for computer-user interfaces using magnetic levitation, U.S. patent number 5,146,566.

Howe, R.D., 1992. A force-reflecting teleoperated hand system for the study of tactile sensing in precision manipulation. In *IEEE International Conference on Robotics and Automation*, Nice, France, pages 1321–1326.

Millman, P., Stanley, M., Grafing, P., and Colgate, J.E., 1992. A system for the implementation and kinesthetic display of virtual environments. In *Proceedings of SPIE–the International Society for Optical Engineering: Telemanipulator Technology*, Boston, MA, pages 49–56.

Minsky, M., Ouh-young, M., Steele, O., Brooks, F.P. Jr., and Behensky, M., 1990. Feeling and seeing: issues in force display. In *Proceedings 1990 Symposium on Interactive 3D Graphics*, pages 235–243.

Mussa-Ivaldi, F.A., Kay, B.A., Hogan, N. and Fasse, E. Perceiving the properties of objects using arm movements: Workspace-dependent effects. In *IEEE Engineering in Medicine and Biology Society, 11th Annual International Conference*, pages 1522–1523, June 1989.

Oh, S.-R., Hollis, R.L., and Salcudean, S.E., 1993. Precision Assembly with A Magnetically Levitated Wrist. In *Proc. IEEE Conf. Robotics Automat.*, Atlanta, USA, pages 127–134.

Ouh-Young, M., Pique, M., Hughes, J., Srinivasan, N., and Brooks, F.P. Jr., 1988. Using A Manipulator for Force Display In Molecular Docking. In *Proc. IEEE Conf. Robotics Automat.*, Philadelphia, USA, pp. 1824–1829.

Salcudean, S.E., Wong, N.M., and Hollis, R.L., 1992. A Force-Reflecting Teleoperation System with Magnetically Levitated Master and Wrist. In *Proc. IEEE Conf. Robotics Automat.*, Nice, France, pp. 1420–1426.

Vlaar, T. D., 1994. Mechanism emulation with a magentically levitated input/output device. Master's thesis, University of British Columbia.

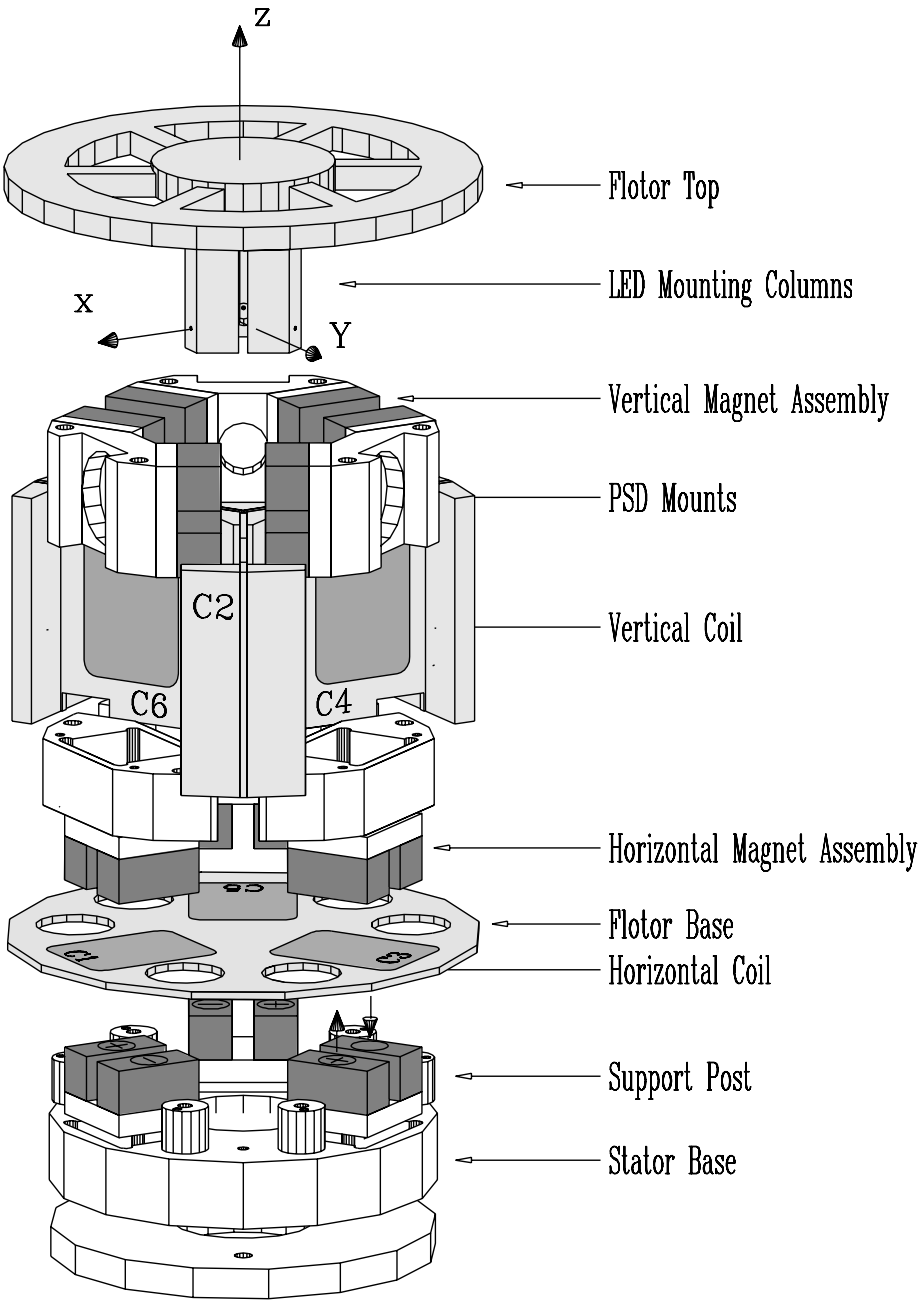

Figure 1: The UBC maglev joystick assembly sketch.

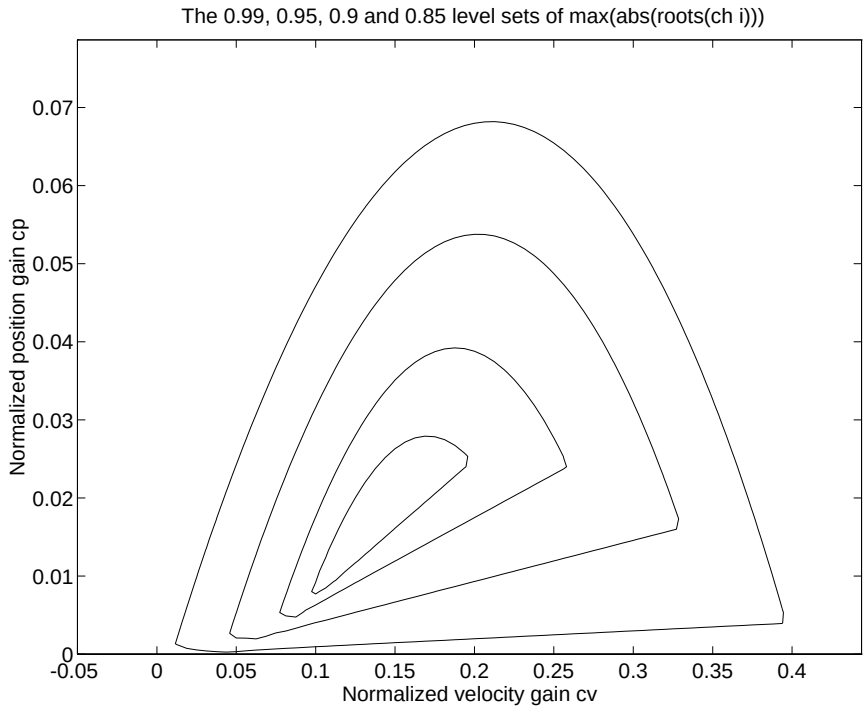

Figure 2: Level sets of the largest magnitude of the roots of χ *vs* non-dimensional coefficients c_p, c_v.

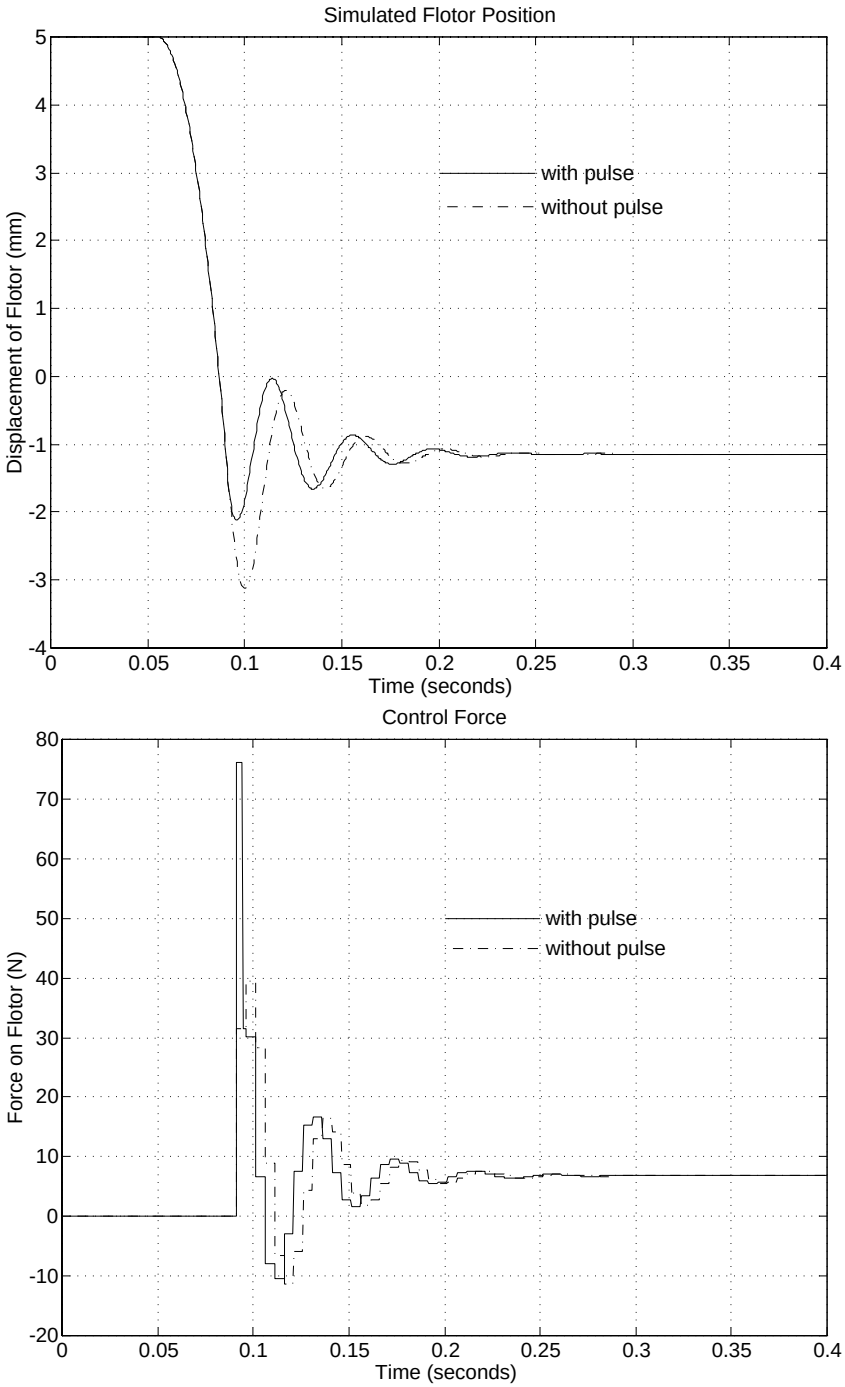

Figure 3: Simulation of the flotor being dropped on emulated hard surface: (a) Flotor position, and (b) control forces. The flotor penetrates the surface less and oscillates less when the braking force pulse is applied.

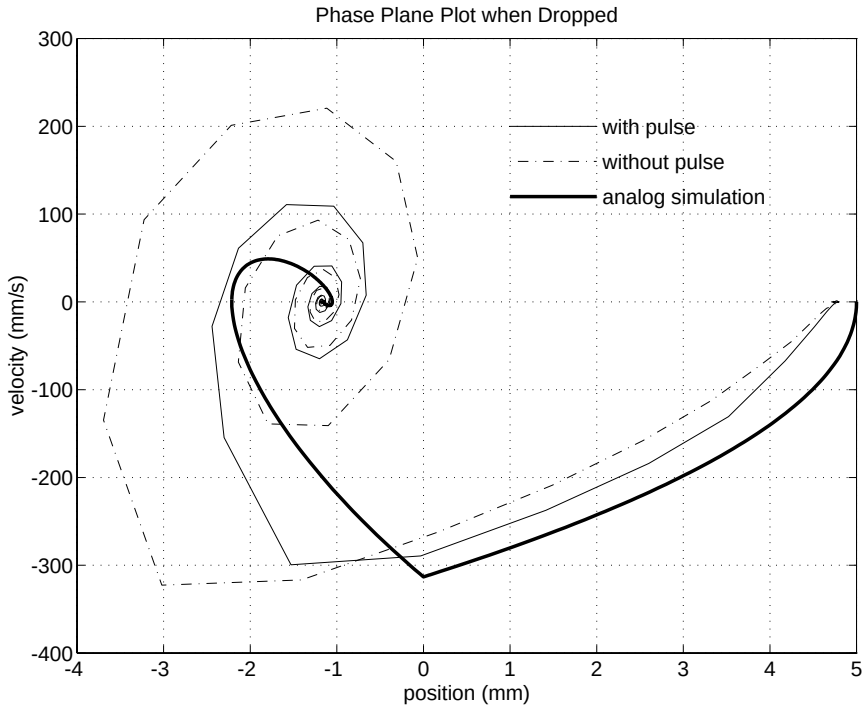

Figure 4: Simulation data showing the velocity *vs* position of the flotor when dropped on emulated stiff wall. The deterioration of performance due to controller discretization and the positive effect of the braking pulse on the discrete controller are clearly displayed.

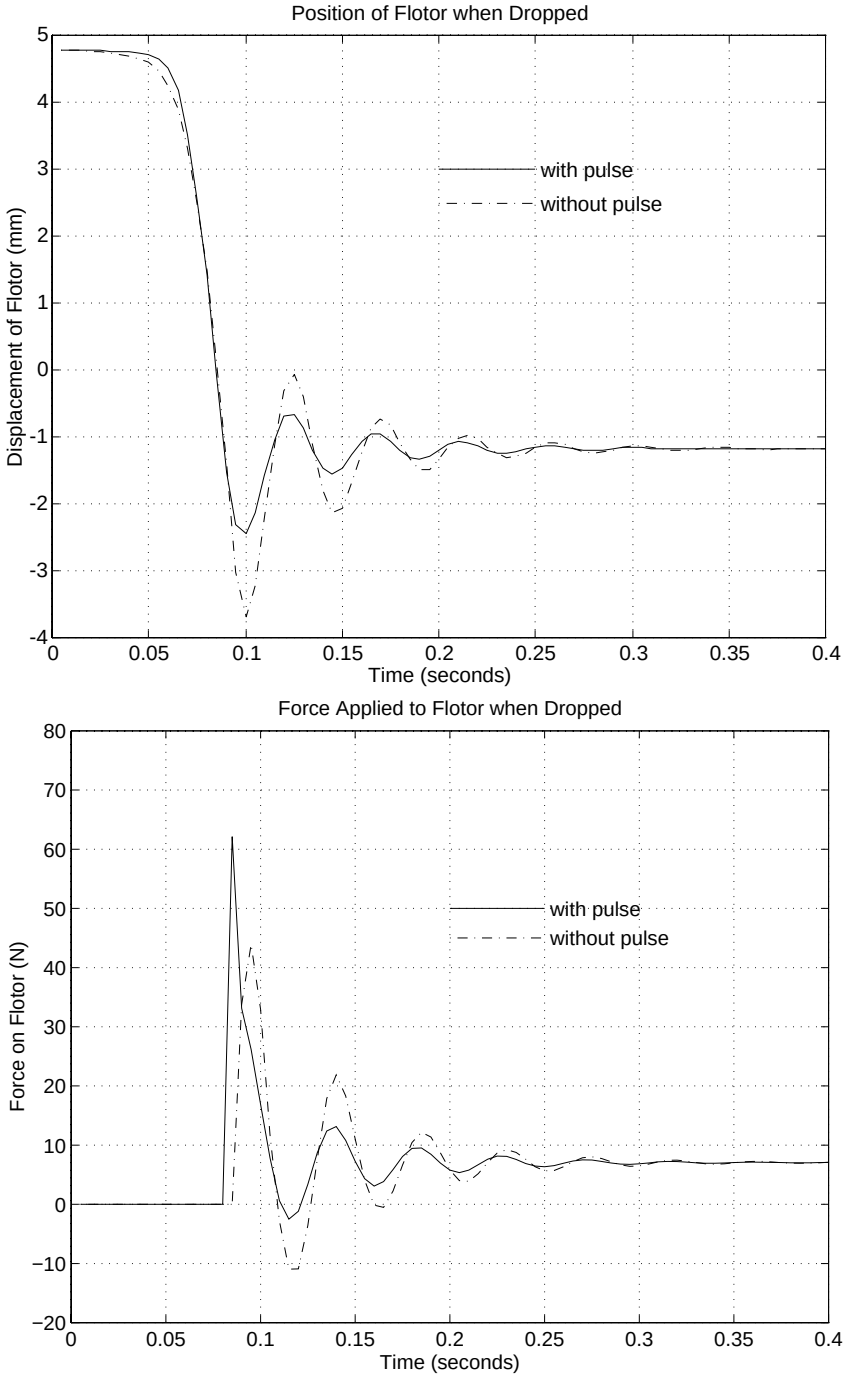

Figure 5: Experimental data showing (a) flotor position, and (b) control forces, when the flotor is dropped on an emulated stiff wall. The flotor penetrates the surface less and oscillates less when the braking force pulse is applied.

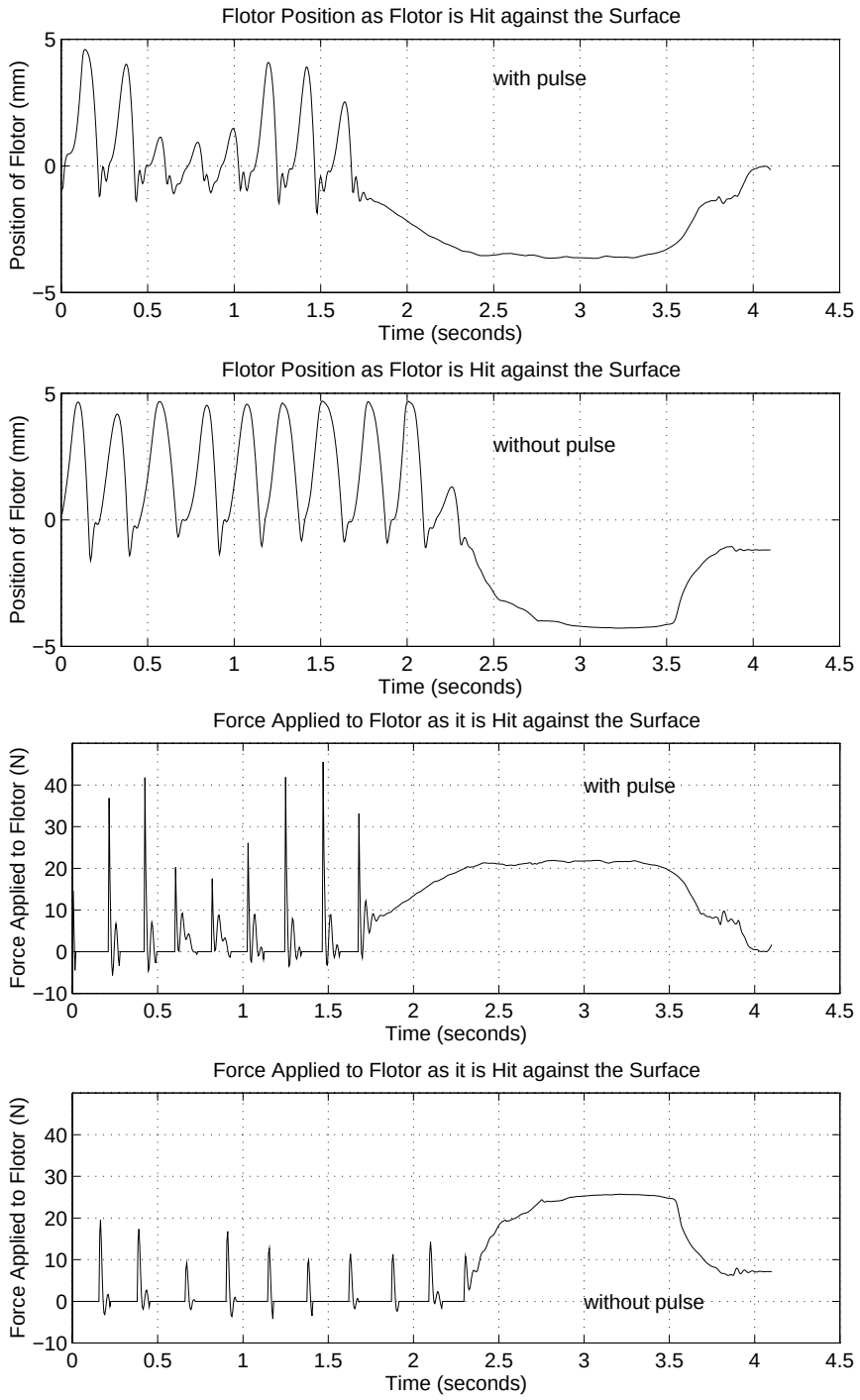

Figure 6: Flotor manipulation: (a) position, and (b) control forces. The operator hits the virtual wall several times, then presses continuously against it.

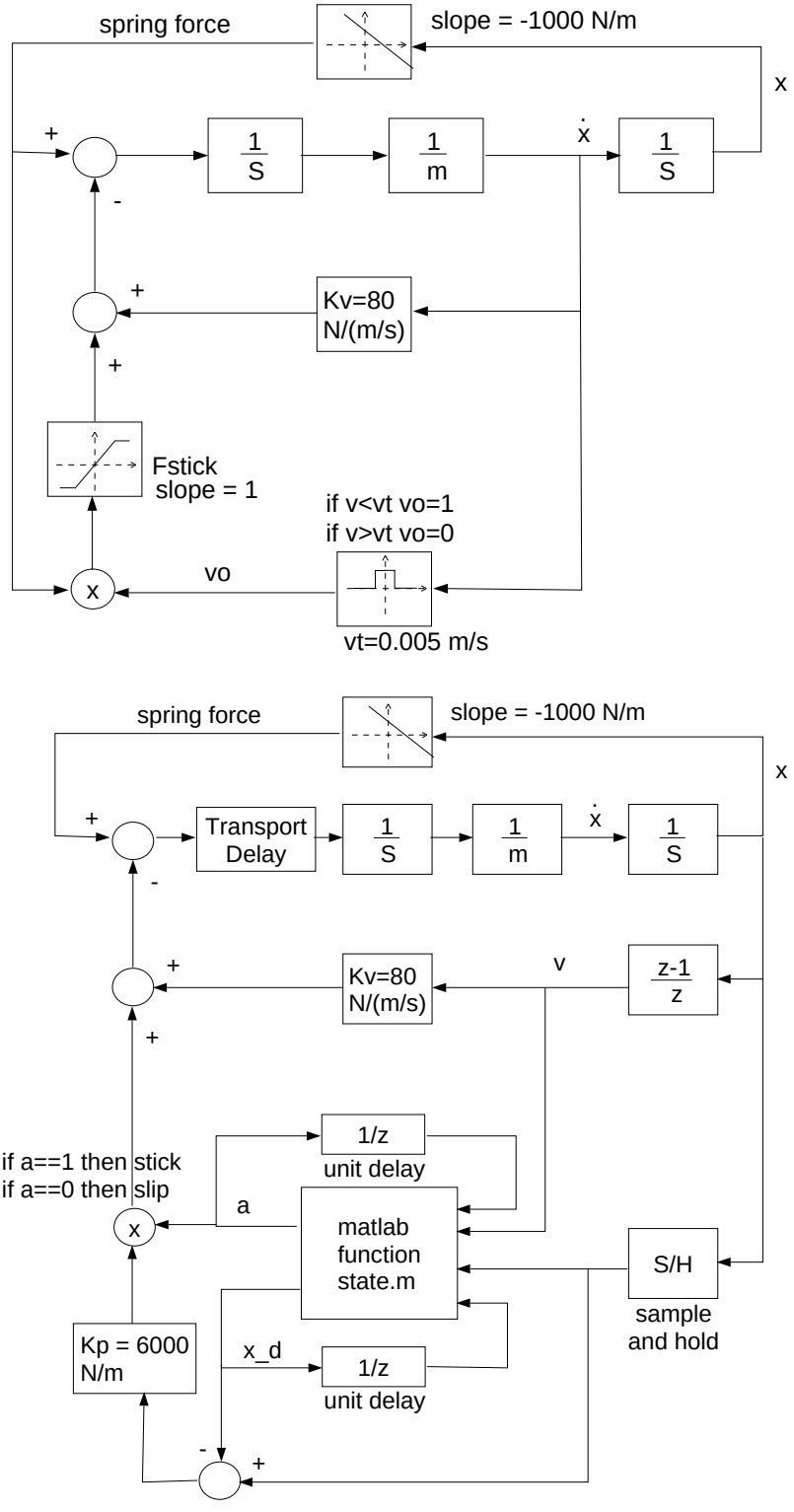

Figure 7: Stick-slip friction model and emulation: a) Karnopp's model, b) digital controller emulation.

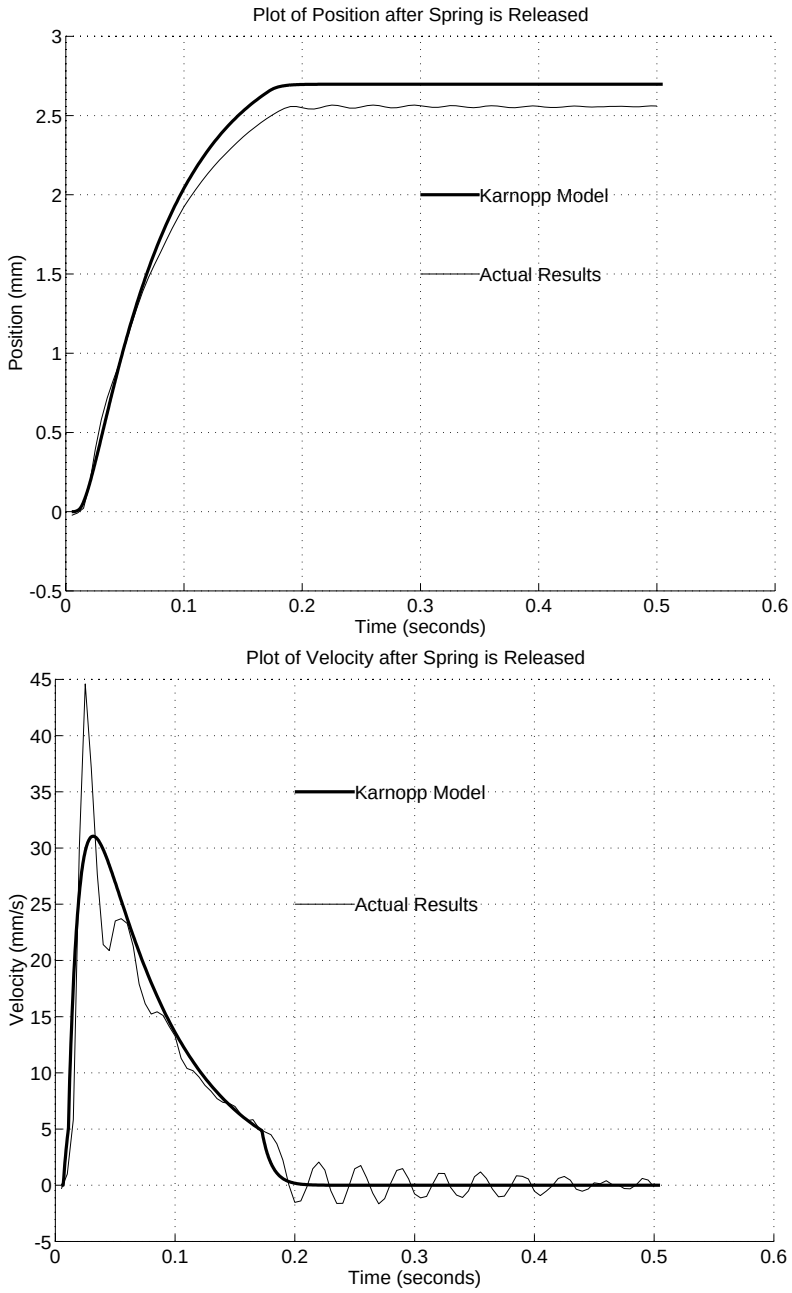

Figure 8: Comparison of the Karnopp model and emulated stick-slip motion of the flotor when pushed by a virtual spring: a) flotor position, b) flotor velocity.

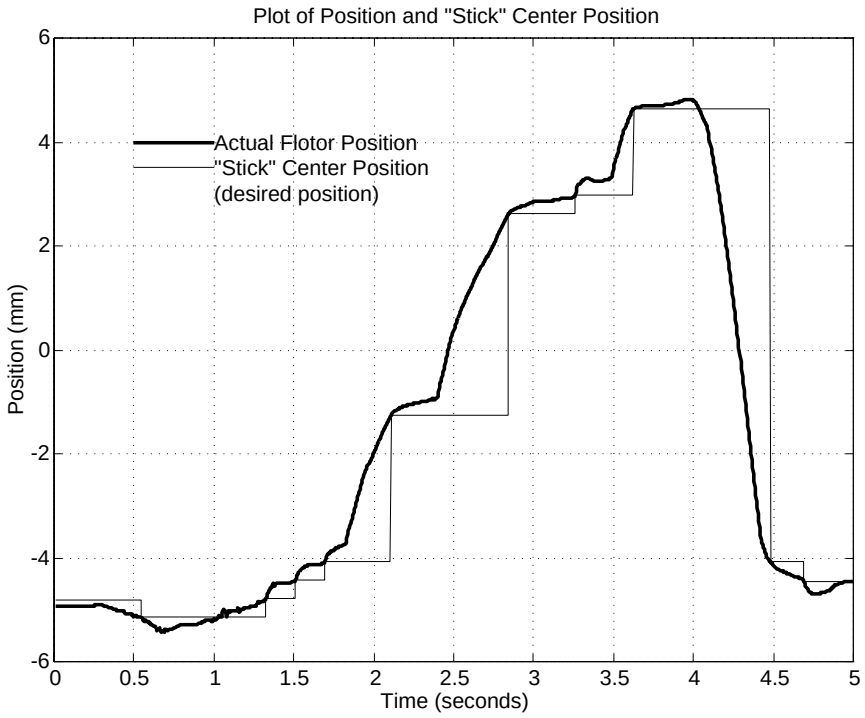

Figure 9: x_{STUCK} set point and actual flotor position when the flotor is manipulated by an operator.